Note on a New Solution of the Taylor-Goldstein Equation and Applications to the Atmosphere

WILLIAM R. MONINGER[1]

Coe College, Cedar Rapids, Iowa 52402

EARL E. GOSSARD

NOAA/ERL/Wave Propagation Laboratory, Boulder, Colo. 80302

8 September 1975 and 8 December 1975

ABSTRACT

A model having smooth wind and density profiles, for which a new solution of the Taylor-Goldstein equation can be found, is described. This model is particularly suitable for comparison with the analogous piecewise linear model so that the influence of "corners" in profiles can be judged. Such corners are found in models studied by Rayleigh, Goldstein, Taylor, Howard, Holmboe, and Gossard.

1. Introduction

Small perturbations in the atmosphere obey the equation (Gossard and Hooke, 1975)

$$\frac{d^2W(z)}{dz^2}+\left[\frac{N^2}{(u-c)^2}-\frac{u''}{u-c}-k^2-\frac{2\Gamma u'}{u-c}-\Gamma^2\right]W(z)=0. \quad (1)$$

In this equation $W(z)=[\rho(z)/\rho_0]^{\frac{1}{2}}w$, where w is the vertical component of the velocity perturbation, ρ the unperturbed density of the fluid, and ρ_0 the density at some reference level. The Väisälä-Brunt frequency squared is represented by $N^2=gd(\ln\theta)/dz$, where θ is the potential temperature. The ambient wind and its second derivative with respect to height z are u and u'', respectively. The phase velocity of the disturbance is c, and

$$\Gamma=(g/2c_s^2)(1-N^2c_s^2/g^2),$$

where c_s is the speed of sound.

When c_s is large, the terms containing Γ are negligible compared with the first term in the coefficient for reasonable values of u'. Eq. (1) then reduces to

$$\frac{d^2W(z)}{dz^2}+\left[\frac{N^2}{(u-c)^2}-\frac{u''}{u-c}-k^2\right]W(z)=0, \quad (1a)$$

which has been studied by Taylor (1931), Goldstein (1931), and many other authors. This approximation is equivalent to the Boussinesq approximation.

An important feature of Eq. (1a) is that the first and second terms in the brackets may become infinite where $u=c$. This problem may be circumvented by requiring that $N^2(z)$ and $u''(z)$ go to zero at the height z_c where $u=c$ (the critical level) rapidly enough to overcome the zeroes in their respective denominators. Alternatively, one may require that $W(z)$ tend to zero more rapidly than $u-c$ does as z_c is approached. In this study we have chosen the former course.

Because we wish our model to represent the earth's atmosphere as nearly as possible, we choose to describe the stratification in terms of potential temperature $\theta(z)$ instead of density $\rho(z)$. For static stability $\theta(z)$ must increase with height. In an atmosphere whose lapse rate is exactly adiabatic $d(\ln\theta)/dz=0$.

2. The model

The profiles we chose for the potential temperature and the ambient wind are

$$\theta=\theta_0\exp\left[N_\infty^2\frac{\Delta H}{g}\left(\frac{z}{\Delta H}-\tanh\frac{z}{\Delta H}\right)\right], \quad (2)$$

$$u=u_\infty\tanh\frac{z}{\Delta H}, \quad (3)$$

where N_∞^2 and u_∞ are the Väisälä-Brunt frequency and ambient wind, respectively, at $z\to\infty$. This model is shown in Fig. 1. Models having a hyperbolic tangent wind profile have been studied by Drazin (1958), Holmboe (1960), and others. This wind profile has simple analytic properties and is a reasonable representation of real shear layers.

We chose Eq. (2) because it is a smooth profile model that can be compared directly with the corresponding piecewise linear model and so can be used to assess the effect of corners on the profile. However, such profiles

[1] This work was carried out while under a temporary appointment at the NOAA/ERL Wave Propagation Laboratory.

may sometimes represent actual atmospheric conditions during the onset of intense mixing associated with a wind discontinuity. The mixing of momentum would tend to erase the shear as well as the gradient of potential temperature in the eventual steady state, but if the shear is maintained by some process external to the model, the profiles might look much like those of our model during the transient thickening of the mixed layer.

The almost linear appearance of θ away from the shear layer is due to the very small (typical atmospheric) value of N_∞^2 in the exponent. In this model

$$N^2 = N_\infty^2 \tanh^2 \frac{z}{\Delta H}, \tag{4}$$

$$u'' = -2\frac{u_\infty}{\Delta H^2} \operatorname{sech}^2 \frac{z}{\Delta H} \tanh \frac{z}{\Delta H}, \tag{5}$$

both of which vanish at $z=0$.

Eq. (1) applies to a two-dimensional disturbance propagating in the x direction. Thus $c=\sigma/k$, where σ is the frequency and k the wavenumber in the x direction. Solutions for which the frequency (and hence the phase speed) is complex will represent unstable perturbations. However, we only seek solutions where c is real because such solutions define the stability boundary [see Miles, (1963) and the discussion below]. In addition, because of the symmetry of the profiles, we assume that $c=0$. In this case, using Eqs. (4) and (5), Eq. (1) becomes

$$\frac{d^2W(z)}{dz^2} + \frac{1}{(\Delta H)^2}\left[\left(\frac{N_\infty}{\beta_0}\right)^2 - \alpha^2 + 2\operatorname{sech}^2\frac{z}{\Delta H}\right]W(z) = 0, \tag{6}$$

where $\beta_0 = u_\infty/\Delta H$ and $\alpha = k\Delta H$.

A solution to Eq. (6) which satisfies the boundary conditions $W(\pm\infty)=0$ is

$$W(z) = A \operatorname{sech}\frac{z}{\Delta H} \tag{7}$$

and

$$\left(\frac{N_\infty}{\beta_0}\right)^2 = \alpha^2 - 1. \tag{8}$$

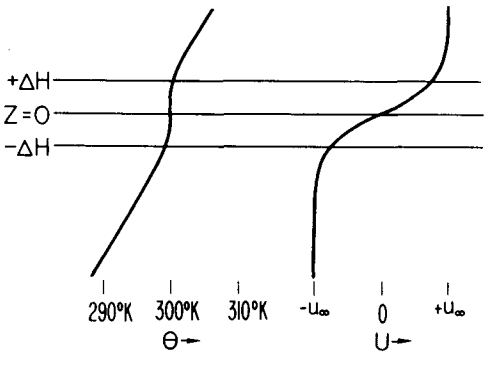

FIG. 1. Wind and potential temperature profiles for this model.

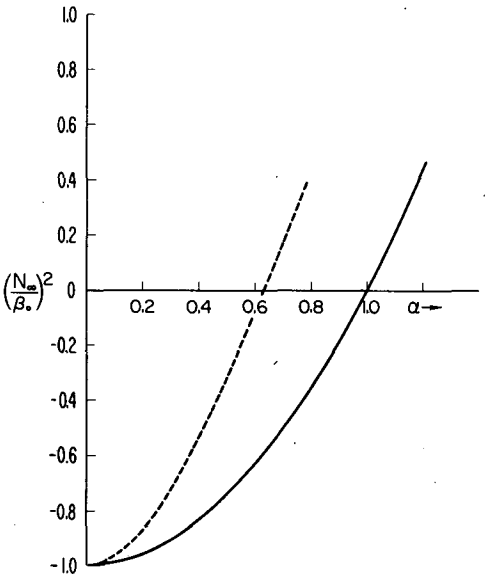

FIG. 2. Neutral curves: solid for this model; dashed for Gossard's three-layer model.

Another solution to Eq. (6) is $W(z)=A\cosh^2(z/\Delta H)$. However, this does not satisfy the boundary conditions and we disregard it. Eq. (8) defines a curve shown as the solid line in Fig. 2. According to an important result of Miles (1963), such a locus of stable solutions in the α, $(N_\infty/\beta_0)^2$ plane implies the existence of a contiguous region of unstable solutions. Eq. (8) thus defines the stability boundary. The unstable region lies above the curve.

3. Comparison with other models

Perhaps the principal practical value of this solution is that it permits us to compare the stability boundary of this model, which has smooth profiles with continuous derivatives, with the stability boundary of the corresponding three-layer, piecewise linear model. This comparison will permit an assessment of the effects of "corners" on the profiles of models such as those of Goldstein (1931), Taylor (1931), Howard (1963), Holmboe (1962) and Gossard (1974). This is important because piecewise linear models can be synthesized that

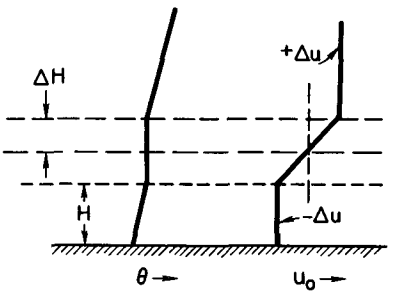

FIG. 3. Wind and potential temperature profiles for Gossard's three-layer model.

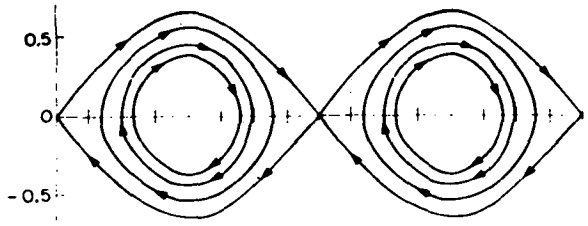

FIG. 4. Streamline pattern for this model.

represent very general conditions including a rigid lower boundary at an arbitrary distance below the shear layer and discontinuities at the edges of the shear layer.

The general eigensolution for a three-layer model, piecewise linear (almost) but continuous in wind and potential temperature and containing a rigid lower boundary, has been given by Gossard (1974). The model is shown in Fig. 3 and the required relation between σ, α in terms of H, ΔH, N_1, N_3 and β is

$$\left[\left(1+\frac{\alpha_1\alpha_3}{\alpha^2}\right)\tanh 2\alpha+\frac{\alpha_1+\alpha_3}{\alpha}\right]\left(\frac{\sigma}{\beta}\right)^2+\left[\left(\frac{\alpha_1-\alpha_3}{\alpha}\right)\tanh 2\alpha\right]\frac{\sigma}{\beta}+(2\alpha-\alpha\alpha_1-\alpha\alpha_3)-(1+\alpha^2-\alpha_1-\alpha_3+\alpha_1\alpha_3)\tanh 2\alpha=0, \quad (9)$$

where

$$\left.\begin{aligned}\alpha_1&=\gamma_1\Delta H\ \mathrm{ctnh}\gamma_1 H\\ \alpha_3&=\gamma_3\Delta H\\ \gamma_1&=k\left[1-\left(\frac{N_1/\beta}{\sigma/\beta+\alpha}\right)^2\right]^{\frac{1}{2}}\\ \gamma_3&=k\left[1-\left(\frac{N_3/\beta}{\sigma/\beta-\alpha}\right)^2\right]^{\frac{1}{2}}\end{aligned}\right\}.$$

The subscripts 1, 3 apply to the lower and upper layers, respectively. N_1 and N_3 are assumed to be constant in the lower and upper layers so the profile of θ is exponential and thus not quite linear above and below the shear layer. However, applied to the real atmosphere, it is very nearly linear in those regions when N is constant. Within the shear layer $N_2=0$.

When $N_1=N_3$, $H=\infty$ and $\sigma/\beta=c=0$, this becomes the three-layer analog of the smooth model we study in this paper. Under these conditions Eq. (9) simplifies to

$$[(\alpha_\infty-1)^2+\alpha^2]\tanh 2\alpha+2\alpha(\alpha_\infty-1)=0, \quad (10)$$

where $\alpha_\infty^2=\alpha^2-(N_\infty/\beta)^2$ and the subscript ∞ designates the value in both layers 1 and 3. The stability boundary plotted from Eq. (10) is shown plotted as the dashed curve in Fig. 2. The general shape is the same as that of the solid curve plotted from Eq. (8). Both curves pass through $(N_\infty/\beta_0)^2=-1$ at $\alpha=0$.

When the model shown in Fig. 3 has a homogeneous density distribution (or $d\theta/dz=0$) it becomes a special case studied by Rayleigh (1945). Then $N_\infty=0$ so $\alpha_\infty=\alpha$ and (10) reduces to the Rayleigh condition for stability:

$$\frac{\tanh 2\alpha}{1+\tanh 2\alpha}-\alpha(1-\alpha)>0, \quad (11)$$

which yields $\alpha>0.64$. Therefore, the stability boundary for the three-layer model passes through 0.64 at $N_\infty/\beta=0$ as seen in Fig. 2.

Two smooth models in which the Richardson number does not vanish at the critical level were analyzed by Drazin (1958) and Holmboe (1960). For density (or, similarly, potential temperature) Drazin uses a simple exponential; Holmboe uses a hyperbolic tangent exponent. For example, the Holmboe function is, in our notation

$$\theta=\theta_0\exp\left[N_0^2\frac{\Delta H}{g}\tanh\left(\frac{z}{\Delta H}\right)\right], \quad (12)$$

where N_0 represents the Väisälä-Brunt frequency at $z=0$. Both Drazin and Holmboe use a hyperbolic tangent wind profile.

The eigensolutions and stability boundaries for both models are similar in form:

$$W(z)=A\left[\mathrm{sech}\left(\frac{z}{\Delta H}\right)\right]^{\epsilon}\left[\tanh\left(\frac{z}{\Delta H}\right)\right]^{1-\epsilon}, \quad (13)$$

$$\left(\frac{N_0}{\beta}\right)^2=\epsilon(1-\epsilon). \quad (14)$$

For the Drazin model, $\epsilon=\alpha^2$; for the Holmboe model, $\epsilon=\alpha$.

Eq. (14) has a maximum at $(N_0/\beta)^2=\frac{1}{4}$ in either model. This is in agreement with a theorem of Miles (1961) and Howard (1961) which states that a sufficient condition for stable fluid flow is that the local Richardson number $[(N/\beta)^2]$ be greater than $\frac{1}{4}$ everywhere in the fluid. The stability boundary curves shown in Fig. 2 exhibit no such limit. This is because $(N/\beta)^2=0$ at $z=0$ and thus the Miles-Howard theorem cannot be satisfied. Instead, the curves increase monotonically as α increases and there is always instability at some α.

Both of the eigenfunctions represented by Eq. (13) become that of our model [Eq. (1)] in the special case of $\alpha=1$. However, our solution and the stability boundary we find are valid for all α's.

At $N_0=N_\infty=0$, corresponding to a homogeneous fluid, or an adiabatic atmosphere, all three smooth models give $\alpha=1$ as the stability boundary. The piecewise linear model, however, yields $\alpha=0.64$, as mentioned earlier. This difference between the smooth and the piecewise linear models is obviously due to the different wind profiles (compare Figs. 1 and 3).

The streamlines for our model resemble the cat's eye pattern that is often seen in radar and acoustic sounder records (see Fig. 4). The Drazin and Holmboe models only yield the cat's eye when $\alpha=1$, which implies an entirely homogeneous atmosphere, i.e., $(N/\beta)^2=0$ (see Howard and Maslowe, 1973).

The cat's eye pattern only occurs when $W(z_c)\neq 0$. This can occur only if all the terms of the Taylor-Goldstein equation [Eq. (1a)] remain finite at $z=z_c$. Thus, the existence of the cat's eye depends critically on the property of our model that $N^2(z_c)=0$, that is, on our assumption of an adiabatic atmosphere at the critical level. Mathematically, this is a very special case, but observationally the cat's eye pattern is a common pattern found in records from many kinds of remote sensors.

A model due to Garcia (1961), $u=u_\infty \tanh(z/\Delta H)$, $\theta=\theta_0 \exp[(\text{const}) \tanh^3(z/\Delta H)]$, also yields the cat's eye and instability for all α. However, in the Garcia model the atmosphere becomes homogeneous at $z=\pm\infty$, i.e., the environment away from the shear layer is nearly homogeneous. Our model may provide some insight as to why the cat's eye pattern is often seen even when the shear layer is imbedded in a non-homogeneous environment.

Fig. 2 also suggests a generalization of a result reported by Gossard and Moninger (1975). They analyzed a fairly complicated model with profiles composed of wind and temperature segments. The model was three-dimensional and included a surface superadiabatic layer, a shear layer, and an inversion capping the shear layer. Because the model contained a superadiabatic layer and a shear layer, two kinds of instability were found—one convective and the other dynamic. Dynamically unstable disturbances were most unstable when aligned transverse to the wind shear, while those disturbances aligned along the shear were most convectively unstable. Both kinds of instability are found in the range $-1<(N_1/\beta)^2(m/k)^2<0$, where N_1 is the Väisälä-Brunt frequency of the superadiabatic layer, β the shear of the shear layer, m wavenumber, and k the component of wavenumber in the direction of shear. Thus this single dimensionless number includes magnitude of stability, shear, and orientation. Only convective instability exists below $(N_1/\beta)^2(m/k)^2=-1$ and only dynamic instability above 0. The cutoff in dynamic instability at -1 was found to be very general and is not affected by the stability of the upper atmosphere or the presence of the capping inversion. The present note demonstrates that this cutoff also does not depend on the "corners" in the profiles of the model. (In the two-dimensional models dealt with here, $m/k=1.0$.)

REFERENCES

Drazin, P. G., 1958: The stability of a shear layer in an unbounded heterogeneous inviscid fluid. *J. Fluid Mech.*, **4**, 214–224.

Garcia, R. V., 1961: Unpublished lecture (see Miles, 1963).

Goldstein, S., 1931: On the stability of superposed streams of fluids of different densities. *Proc. Roy. Soc. London*, **A132**, 524–548.

Gossard, E. E., 1974: Dynamic stability of an isentropic shear layer in a statically stable medium. *J. Atmos. Sci.*, **31**, 483–492.

——, and W. H. Hooke, 1975: *Waves in the Atmosphere*. Elsevier, 456 pp.

——, and W. R. Moninger, 1975: The influence of a capping inversion on the dynamic and convective instability of a boundary layer model with shear. *J. Atmos. Sci.*, **32**, 2111–2124.

Holmboe, J., 1960: Unpublished lecture notes (see Miles, 1963).

——, 1962: On the behavior of symmetric waves in stratified shear layers. *Geophys. Publ.*, **24**, No. 2, 67–113.

Howard, L. N., 1961: Note on a paper of John W. Miles. *J. Fluid Mech.*, **10**, 509–512.

——, 1963: Neutral curves and stability boundaries in stratified flow. *J. Fluid Mech.*, **16**, 333–342.

——, and S. A. Maslowe, 1973: Stability of stratified shear flows. *Bound.-Layer Meteor.*, **4**, 511–523.

Miles, J. W., 1961: On the stability of heterogeneous shear flows. *J. Fluid Mech.*, **10**, 496–508.

——, 1963: On the stability of heterogeneous shear flows, Part. 2. *J. Fluid Mech.*, **16**, 209–227.

Rayleigh, J. W. S., 1945: *The Theory of Sound*, Vol. 2 (reprint of 2nd ed. of 1896). Dover, Chap. 21.

Taylor, G. I., 1931: Effect of variation in density on the stability of superposed streams of fluid. *Proc. Roy. Soc. London*, **A132**, 499–523.